

**MINERAL AND FLUID EQUILIBRIA IN Mo-BEARING SKARN
AT THE ZENITH DEPOSIT, SOUTHWESTERN GRENVILLE PROVINCE,
RENFREW AREA, ONTARIO, CANADA**

STEFANO SALVI[§]

*Laboratoire des Mécanismes de Transfert en Géologie, UMR 5563, Equipe de Minéralogie,
Université Paul-Sabatier, 39, Allées Jules Guesde, F-31000 Toulouse, France*

ABSTRACT

Late-tectonic pegmatitic, aplitic and graphic granites intrude metasedimentary units of the Grenville Supergroup, Composite Arc Belt, in the Renfrew area of southeastern Ontario. Zoned molybdenite-bearing skarns occur at the contact of graphic pegmatites with mixed calcite–dolomite marble, para-amphibolite and gneiss at the Zenith molybdenite deposit. Distal skarns also are found, in the form of discordant veins within foliated marble. Mineral zoning in the skarn consists of diopside–microcline endoskarn plus exoskarn that grades, away from the intrusion, from a diopside-dominant to a tremolite-dominant metasomatic rock. Textural evidence indicates that tremolite was an earlier-formed skarn mineral in the diopside zone. Diopside is absent in the tremolite zone. These patterns are repeated in other similar occurrences of skarn in the area. Apatite grains formed during metasomatism contain primary high-salinity (≥ 30 wt.% NaCl eq.) liquid-rich fluid inclusions coexisting, along growth zones, with vapor-rich inclusions, indicative of the trapping of an immiscible fluid. The observed parageneses are interpreted to reflect metasomatic replacement of marble by infiltration of a silica-rich orthomagmatic fluid that evolved by the crystallization of the granitic pegmatite, at approximately 600°C and 300 MPa. Such conditions are not inconsistent with phase separation of the aqueous fluid, because the salinity of the fluid is known to drastically raise the critical temperature of the H₂O–CO₂ miscibility gap. A decrease in temperature or in the chemical potential of silica in skarn furthest from the granites (or both) may account for formation of the tremolite zone. The Mo likely was transported in the metasomatic fluid as alkali oxyacidic complexes. A decrease in $f(\text{O}_2)$ along with reduction of magmatic sulfur upon interaction of the fluid with graphite-bearing marble are inferred to have triggered the precipitation of molybdenite.

Keywords: skarn, molybdenite, hydrothermal, metasomatism, fluid immiscibility, fluid inclusions, Zenith deposit, Composite Arc Belt, Grenville Province, Ontario.

SOMMAIRE

Des venues post-tectoniques de granite à texture graphique, aplitique ou pegmatitique recoupent les unités métasédimentaires du Supergroupe du Grenville, au sein de la Ceinture d'Arcs Composite dans la région de Renfrew, secteur sud-est de l'Ontario. Le gisement de Zénith comprend des skarns zonés et minéralisés en molybdénite, développés au contact des pegmatites graphiques avec des marbres à calcite et dolomite. Des skarns distaux forment aussi des veines discordantes dans le marbre. Les skarns présentent une zonation minéralogique, avec des endoskarns à feldspaths et diopside, et des exoskarns composés surtout de diopside. En s'éloignant du contact intrusif, on trouve des skarns à dominance de trémolite. Une étude des textures montre que dans la zone à diopside, la trémolite a été remplacée par ce minéral. Par contre, on ne trouve pas de diopside dans la zone à trémolite. Ces faciès existent aussi dans d'autres skarns dans la région. L'apatite formée pendant la métasomatose contient des inclusions fluides salines ($\geq 30\%$ NaCl eq., en poids) riches en liquide; elles coexistent, le long des fronts de croissance, avec des inclusions riches en vapeur. Cette coexistence indique que le fluide était sous-critique lors du piégeage. La paragenèse observée dans les skarns est probablement due à un ré-équilibre du marbre en réponse à l'introduction d'un fluide orthomagmatique enrichi en silice issu de la cristallisation des pegmatites, à environ 600°C et 300 MPa. Ces conditions ne sont pas incompatibles avec une séparation de phases du fluide, car la salinité élevée augmente la température du point critique de la région d'immiscibilité du système H₂O–CO₂. Une baisse en température ainsi qu'une diminution de l'activité en silice du fluide peuvent être responsables de la formation de la zone à trémolite dans les skarns les plus éloignés des granites. Le molybdène aurait été transporté dans le fluide sous forme de complexes oxyacidiques. Une chute de la fugacité d'oxygène et une augmentation de l'activité de H₂S, due à la réduction du soufre magmatique lors de l'interaction du fluide avec le marbre à graphite, auraient déclenché la précipitation de la molybdénite.

Mots-clés: skarn, molybdénite, hydrothermale, métasomatose, immiscibilité des fluides, inclusions fluides, gisement de Zénith, Ceinture d'Arcs Composite, province du Grenville, Ontario.

[§] E-mail address: salvi@cict.fr

INTRODUCTION

Although skarns represent a very small volume percentage of crustal rocks, they have received a great deal of attention by researchers over the years, largely owing to their association with ore deposits (Au, Cu, Fe, Mo, Sn, W, and Zn–Pb) (*e.g.*, Zharikov 1970, 1991, Einaudi *et al.* 1981, Burt 1982, Ray & Webster 1991, Meinert 1992, 1997, Lentz 1998a). Of these, molybdenum-bearing skarns are probably the least studied. The majority of Mo skarns found in Precambrian shields are associated with leucocratic aplitic and pegmatitic granites and occur in carbonate rocks (Vokes 1963). The southwestern part of the Composite Arc Belt, formerly the Central Metasedimentary Belt of the Grenville Province in Ontario contains numerous examples of U, Th, Mo and rare-earth element (*REE*) mineralization hosted by skarns, vein-dikes and pegmatites (*e.g.*, Satterly 1957, Vokes 1963, Johnston 1968, Karvinen 1973, Malczak *et al.* 1985, Lentz 1991, 1996, 1998b, Lentz & Suzuki 2000). Several of these showings have been mined in the past or are potentially exploitable. In the study area, near Renfrew, Ontario, molybdenite production took place mainly during the two world wars, whereas radioactive minerals were mined in the mid-1950s and between 1970 and the early 1980s. Between 1915 and 1943, the Zenith deposit produced a few hundred tonnes of ore grading from 0.85 to 5% MoS₂ (*cf.* Carter *et al.* 1980). Although the property was prospected for U and Th in the mid-1950s, these commodities were never exploited.

Reported here are the results of a field, mineralogical and reconnaissance fluid-inclusion study of the Zenith molybdenite-bearing skarn. To compensate for the limited exposure, a number of similar types of mineralization were also visited: the Hunt, Spain and Sunset Mo deposits, as well as two road-cut exposures. In this paper, I attempt to explain the mineralogical patterns and skarn formation. The skarn terminology follows the recommendations of Einaudi & Burt (1982).

GEOLOGICAL SETTING

The Zenith deposit is located 13.3 km south of Renfrew, Ontario (lat. 45°23'33", long. 76°42'20"). This deposit and the other skarn occurrences studied are found within the Bancroft and Renfrew map sheets 2461 and 2462 (Lumbers 1982; Fig. 1). According to the lithotectonic reinterpretation of the Grenville Province by Carr *et al.* (2000), these occurrences of mineralization occur within the northern part of the Belmont Domain of the Composite Arc Belt (see also Easton 2000). This domain comprises metavolcanic and metasedimentary rocks of the Grenville Supergroup, deposited largely between 1300 and 1200 Ma (Easton 2000, and references therein), as well as early- to late-tectonic plutonic suites (*e.g.*, Davidson 1986). Within the Composite Arc Belt, the Grenvillian orogenic cycle, which

culminated with the Ottawa orogeny (*ca.* 1090–1100 Ma; Easton 1986), caused units of the Belmont Domain to be intensely deformed. Metamorphism in the northern part of the Belmont Domain reached upper amphibolite grade (Wynne-Edwards 1972, Easton 2000). Granitic pegmatites in the area give Rb–Sr whole-rock ages of *ca.* 980 Ma (Fowler & Doig 1983), although these are now interpreted to be closure ages; emplacement is considered to have taken place between 1060 and 1010 Ma (Lentz 1991).

The Zenith deposit occurs in a calcareous metasedimentary succession of amphibolite grade contained as xenoliths within the western margin of the deformed Hurd Lake Trondhjemite (Fig. 1). The trondhjemite cross-cuts the country rock, which consists of interbedded marble, calc-silicate metasediments and quartzofeldspathic gneiss. Exposure in the area is poor, but near the main shaft, an intercalated package of marble and gneiss units is well exposed (Fig. 2, inset), showing north-northeasterly strike and a steep westward dip. As observed in one of the trenches that were dug during mining operations, tight isoclinal folds are refolded by gentle folds plunging shallowly to the southwest; a faint subhorizontal axial-planar cleavage is related to the latter structure. Both metagranitic and metasedimentary rocks are cut by a pegmatitic granite. At the contact of the pegmatitic granite with the marble, discontinuous, relatively short and narrow lenticular bodies of skarn are developed; Quinn (1952) reported a typical size for a skarn lens to be about 15 by 5 meters.

Several rock units were recognized at the Zenith deposit (Fig. 2). Cross-cutting relationships indicate that the oldest rocks are a metasedimentary sequence consisting of quartzofeldspathic, calc-silicate, and calcitic to dolomitic units. The quartzofeldspathic gneiss is fine- to medium-grained, white to pink with very well-defined bands 1–2 cm thick, reflecting variations in feldspar and biotite + hornblende contents. The well-foliated calc-silicate metasedimentary unit is fine grained and dark brown in color. Compositional banding of less than cm scale can be observed on the weathered surface. Garnet porphyroblasts mark Al-rich layers; predominant mafic minerals are biotite and hornblende, with minor clinopyroxene. The amphibolite is dark colored, fine to medium grained, and is mainly composed of plagioclase, biotite and hornblende. Marble in the area is a medium- to coarse-grained, light-colored rock that occurs as thin units intercalated with the other metasedimentary rocks; it is made up of subequal proportions of calcite and dolomite, plus accessory amounts of phlogopite, tremolite, graphite and, locally, sulfides.

The foliated granitic rock attributed to the Hurd Lake Trondhjemite is light gray, fine grained (1 mm), and consists of feldspars (70%), quartz (10 to 20%) and biotite (≤5% to enriched pods containing up to 20%). In places, biotite is replaced by magnetite and occasionally occurs as veinlets that parallel the foliation as well as extensional fractures perpendicular to them. This

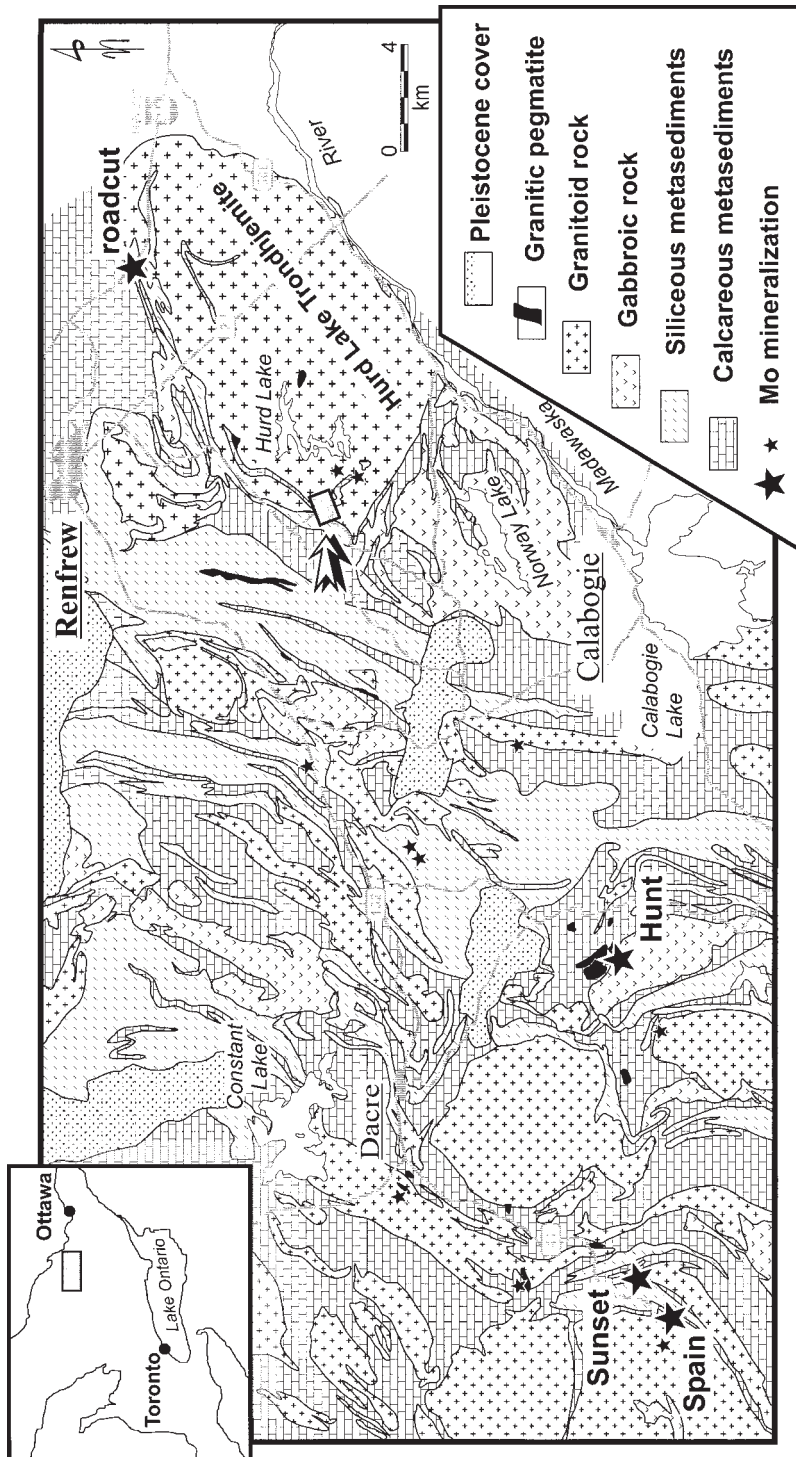


FIG. 1. Regional geology and location of the Zenith deposit (arrow) and other Mo-skarn deposits (stars) visited, as modified after Quinn (1952) and Lumbers (1982). The small, unlabeled stars indicate other Mo-bearing (\pm U) skarn occurrences (from Carter *et al.* 1980).

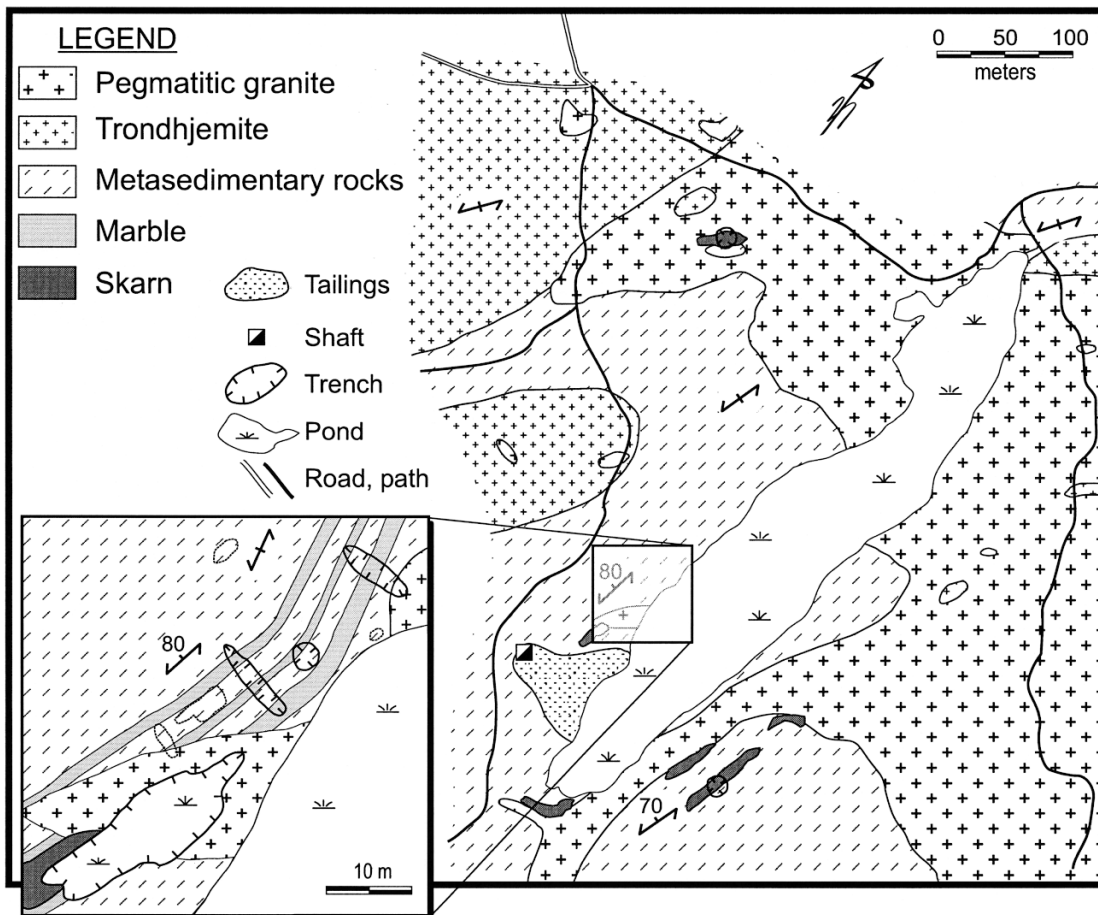


FIG. 2. Simplified surface geology of the Zenith deposit.

metatrandhjemitic body cross-cuts the metasedimentary rocks, but a subvertical foliation in the two units is parallel, suggesting that emplacement took place before or during the last episode of Grenvillian deformation.

The unfoliated pink to red pegmatitic granite is composed mainly of microcline (optically determined; 40%), albite (35%), quartz (20%), and locally biotite and magnetite (<1%). It has a variable grain-size, ranging from aplite through medium- and coarse-grained granite to pegmatite; a graphic texture also is observed. Generally, the pegmatites are concentrated along the margins of the intrusive dykes, in contact with the country rock.

DESCRIPTION OF THE SKARN

Field observations and detailed mapping have revealed the occurrence of two main types of skarn: 1) proximal skarn, comprising endoskarn and exoskarn,

which develop along the pegmatite contact with marble (remarkably well exposed at the Hunt deposit; maps in Carter *et al.* 1980, Lentz & Suzuki 2000), and 2) distal skarn, developed in marble but not found in direct contact with the pegmatite, possibly along pre-existing fractures in the country rock (vein skarn). The skarn has an overall medium green color, is coarse to very coarse grained, and is mineralized with disseminated flakes of molybdenite that range from 1 to 5 cm across. Pyrite and pyrrhotite also are present, but without magnetite. Fe sulfides are more abundant toward the granite contact, whereas molybdenite occurs in both proximal and distal skarn. Locally, the gneiss also has been metasomatized, taking on a light green color but retaining its fine grain-size and original foliation.

Although the skarn typically cross-cuts the granitic pegmatites, at the Spain deposit a pegmatite locally intersects distal Mo-U mineralized veins in the gneisses, indicating a penecontemporaneous origin of the

pegmatites and the skarn. However, this observation led Karvinen (1973) to hypothesize a metamorphic–metasomatic (*i.e.*, premagmatic) origin of the skarn.

Mineralogical zonation in the skarns

In the occurrences studied, zoning is not ubiquitous and commonly difficult to observe in outcrop. Nonetheless, by compiling various pieces of information, a typical pattern of zonation has been established (Fig. 3). Endoskarn forms at the immediate intrusive contact of the pegmatitic granite with marble, and is well exposed in a trench at the Zenith deposit. This zone is typically only a few tens of cm in thickness and consists of variable proportions of K-feldspar, plagioclase and ferroan diopside.

The principal constituent of the exoskarn is coarse grained, commonly monomineralic, medium-green diopside. This is the most abundant type of skarn in the deposits, and has a maximum thickness of about 5 m (Quinn 1952). Diopside forms large crystals (up to 30 cm across), commonly with a radiating texture (Fig. 4). In thin section, it almost invariably shows numerous small inclusions of tremolite. Under crossed nicols, these inclusions all go to extinction at the same position upon rotation of the microscope stage (Fig. 5A); this texture suggests that the tremolite inclusions represent earlier-formed crystals that have been replaced by diopside. Pure white diopside crystals have been observed in distal skarn. Table 1 gives compositions of proximal (green) and distal (white) diopside.

In skarn further away from the intrusive unit, tremolite is the main mineral phase, plus minor amounts of carbonate or quartz. At the Sunset deposit, the pegmatitic granite was not found, although poor exposure could

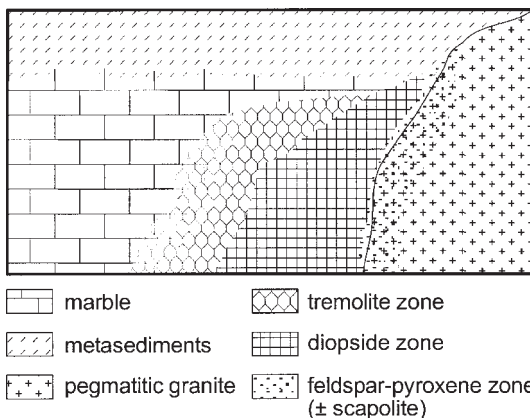


FIG. 3. Schematic cross-section showing skarn zonation developed in marble at an intrusive contact.

account for the apparent absence of such dykes. The large amounts of tremolite present suggest that the Sunset could be a distal skarn occurrence. Figure 5F shows a sample of distal skarn (SZ-16) displaying a zonation from diopside to tremolite and to marble at a cm scale (see also Fig. 6).

Locally, scapolite can be observed in the endoskarn as well as in proximal exoskarn, whereas titanite and ferroan phlogopite, although rare, may occur in proximal exoskarn, with green (Fe-rich) diopside. Apatite occurs as an accessory phase in exoskarn, both in the diopside- and (less commonly) tremolite-dominant zones. It forms relatively small (on average 1×0.5 mm), subhedral to euhedral grains, and shows triple

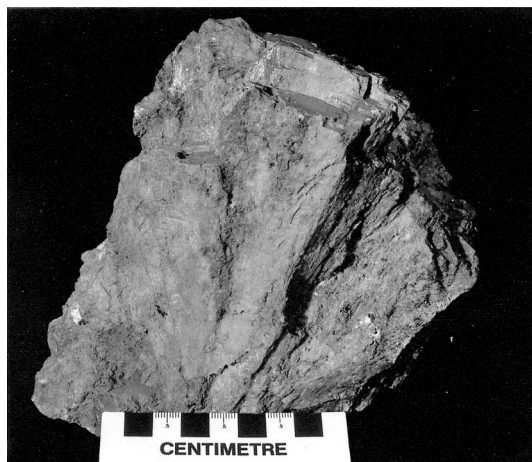


FIG. 4. Coarse-grained radiating diopside from proximal exoskarn at the Zenith deposit.

TABLE 1. COMPOSITION OF THE GREEN AND WHITE DIOPSIDE FROM THE ZENITH DEPOSIT, RENFREW AREA, ONTARIO

	green	white		green	white
SiO ₂ wt. %	54.17	55.85	Si <i>apfu</i>	1.99	2.00
TiO ₂	0.02	0.00	Ti	0.00	0.00
Al ₂ O ₃	0.68	0.11	^{IV} Al	0.01	0.00
			^V Al	0.02	0.00
Cr ₂ O ₃	0.00	0.01	Cr	0.00	0.00
Fe ₂ O ₃ *	1.62	0.23	Fe ³⁺	0.04	0.01
FeO*	4.13	0.32	Fe ²⁺	0.13	0.01
MnO	0.25	0.05	Mn ²⁺	0.01	0.00
MgO	14.60	18.26	Mg	0.80	0.98
CaO	24.04	25.74	Ca	0.95	0.99
Na ₂ O	0.77	0.09	Na	0.05	0.01
K ₂ O	0.00	0.01	K	0.00	0.00
Sum	100.29	100.67	Sum cations	4.00	4.00
Wo %	50.53	50.09			
En %	42.69	49.43			
Fs(Fe ²⁺) %	6.78	0.48			
X _{Mg}	0.86	0.99			

Structural formulae based on six atoms of oxygen. Green diopside: average result of three analyses. White diopside: average result of ten analyses. * : calculated value.

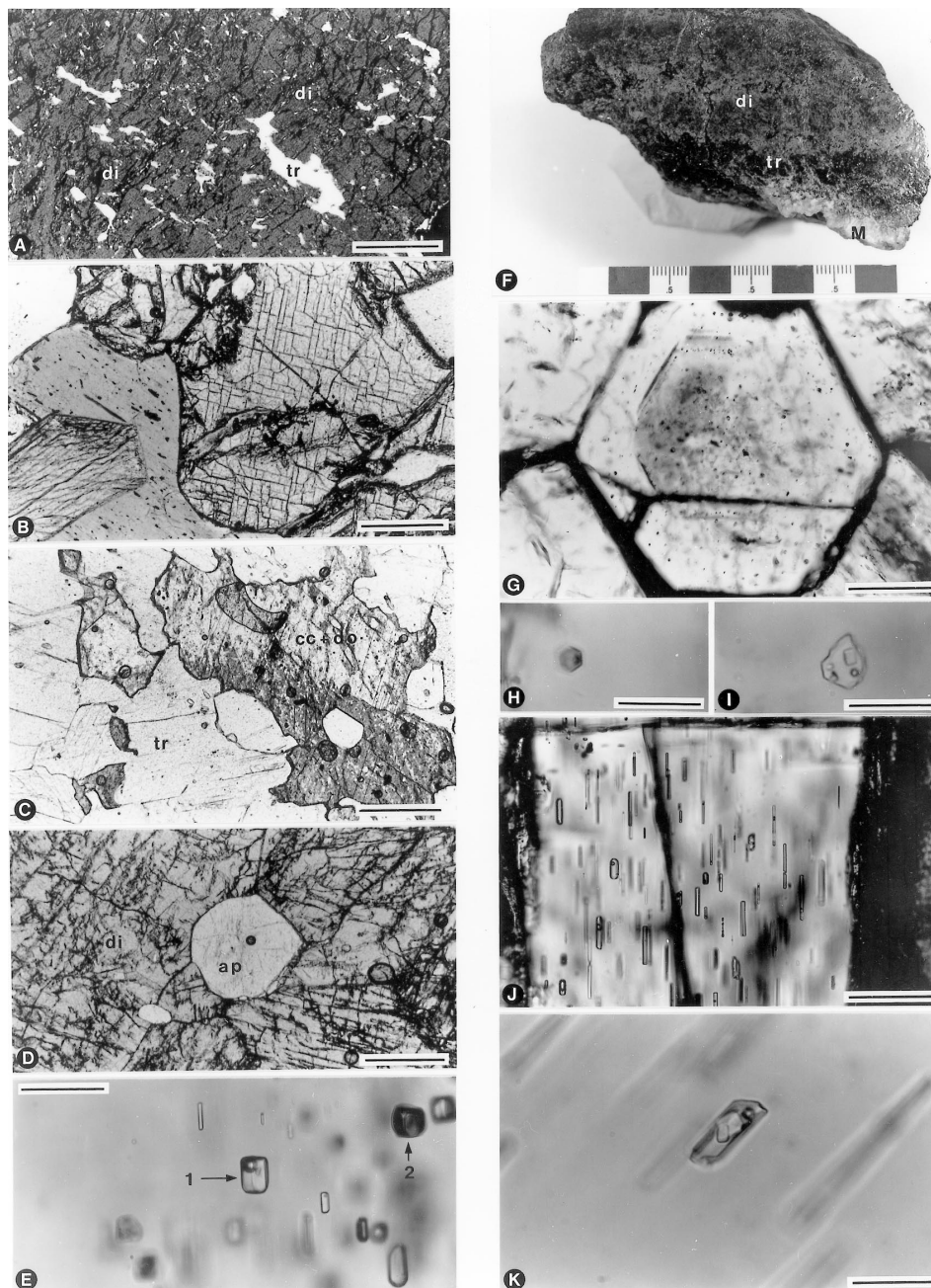


FIG. 5. A. A diopside grain with inclusions of tremolite in optical continuity. B. Diopside zone. C. Boundary between tremolite zone and marble (dolomite is stained) in sample SZ-16. D. Apatite and diopside coexisting, in granoblastic assemblage. E. Fluid inclusions in apatite (1: liquid + vapor + Fe-oxide; 2: vapor-rich). F. Sample SZ-16 showing mineral zonation in distal skarn (di = diopside zone, tr = tremolite zone, M = marble). G. Basal section through a crystal of apatite displaying zoning defined by fluid inclusions. H. Negative-crystal-shaped and I) multiphase inclusions from G. J. Longitudinal section through an apatite grain showing fluid inclusions oriented parallel to the *c* axis of the host crystal. K. Multiphase fluid inclusion from J (isometric solids in I and K are NaCl). All photos in plane-polarized light except A, in crossed polars. Scale bars: A to D: 1 mm, E: 62.5 μ m, F: in cm, G: 250 μ m, J: 125 μ m, H–I–K: 25 μ m.

junctions with other skarn minerals (Fig. 5D). This textural evidence suggests that the apatite crystallized during skarn formation. The very low phosphorus content found in unaltered marbles of the area (0.07 ± 0.15 wt.%, $n = 1778$; cf. Grant *et al.* 1989) is consistent with a metasomatic origin of the apatite. A noticeable characteristic of the skarn studied is the lack of garnet. Although it is a very common aluminosilicate in skarns (*e.g.*, Kerrick 1977, Einaudi *et al.* 1981, Meinert 1992), magnesian skarns typically do not contain garnet. The field of stability of grossular can be overstepped by scapolite stability (*cf.* Lentz 1998b, Pan 1998), and the low $f(\text{O}_2)$ indicated by the opaque mineral assemblage favors crystallization of ferroan diopside over andradite (Gamble 1982, Lentz 1998b).

FLUID INCLUSIONS

Accessory apatite found in these skarns commonly display well-developed growth zones, which are defined by trapped impurities and fluid inclusions (Fig. 5G). As discussed above, the apatite is interpreted to be a primary skarn mineral; the fluid inclusions that were trapped along these growth zones are, therefore, interpreted to contain the skarn-forming fluid. The inclusions are small ($<10 \mu\text{m}$) and have negative crystal shapes. In addition to those defining growth zones, other fluid inclusions occur dispersed within the single crystals of apatite. These are relatively large with respect to the host grain (10 to $100 \mu\text{m}$), *i.e.*, a diameter up to 0.1 that of the crystal, which is one of the criteria listed by Roedder (1984) for distinguishing primary fluid inclusions. Other evidence for a primary origin of these inclusions include their abundance and random distribution within the host mineral. In addition, they have similar shapes and contain the same phases as the inclusions that define the growth zones. Both populations thus are of the same generation. The inclusions vary significantly in shape, but this is easily explained by the tendency of primary inclusions to orient themselves parallel to the *c* axis of the host crystal, especially in apatite (Roedder 1984). Therefore, basal sections of apatite will yield hexagonal inclusions (Figs. 5G–H). Any section cut parallel to the *c* axis or at an oblique angle to it will display inclusions with more or less elongate shapes (Figs. 5J–K). Trains of inclusions can occasionally be found oblique to the crystallographic directions of the apatite grains, and commonly extend beyond grain boundaries; these inclusions are thus regarded as secondary. Morphologically, they are distinct from the inclusions recognized as primary, as they do not have negative crystal shapes.

A wide variety of types of primary inclusions are present within the same grain of apatite (Figs. 5D, 7). These were grouped into the following types of inclusions: type I: liquid-rich; type II: vapor-rich; type III: solid-bearing, three-phase or multiphase inclusions. The liquid-to-vapor ratio in type-I and type-II inclusions defines a continuum, from liquid-filled type-I to vapor-

filled type-II inclusions. The solids contained in type-III inclusions commonly include a cube of halite (recognized on the basis of optical properties), plus birefringent solids (sulfates or chlorides?) and, on one occasion, a red to orange grain that could be a Fe-oxide (hematite?). Although solid-bearing inclusions commonly have small vapor bubbles, their liquid to vapor ratio is not constant.

The presence of primary, coexisting liquid-rich and vapor-rich inclusions can be explained by trapping aliquots of immiscible phases of a subcritical fluid. During phase separation, dissolved salt constituents are preferentially partitioned into the liquid phase. Thus, type-III inclusions likely represent the denser, more saline liquid. The fact that not all liquid-rich inclusions contain solids (*i.e.*, type I) and that size and number of the solids contained in type-III inclusions vary, indicates that the solids were probably trapped.

Reconnaissance microthermometric analyses were performed on a few samples from the Zenith and the Spain deposits, using a Fluid Inc. adapted U.S.G.S. gas-flow heating-freezing stage (Werre *et al.* 1979) calibrated using synthetic fluid inclusions supplied by SYNFLINC. Measurements of inclusions from the two deposits do not differ appreciably. Upon heating, most inclusions decrepitated before homogenization, at a temperature close to 350°C . Decrepitation is consistent with the presence of dissolved, high-density gases (*e.g.*,

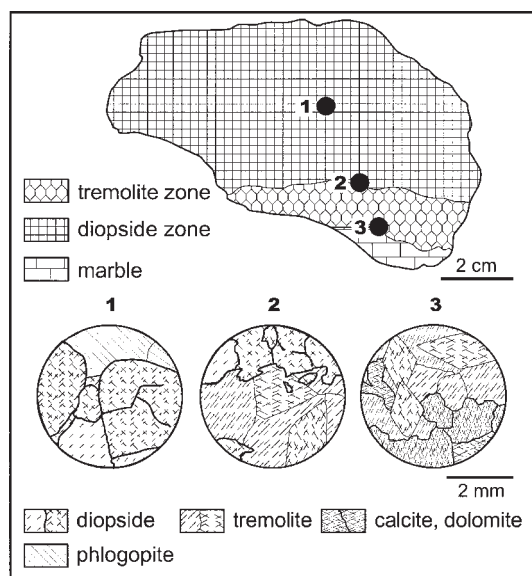


FIG. 6. Map of the mineral zonation in sample SZ-16 (Fig. 5F). Solid circles indicate the location (not to scale) of inset 1 (diopside zone), 2 (contact between diopside and tremolite zones), and 3 (tremolite zone grading into unmetasomatized marble).

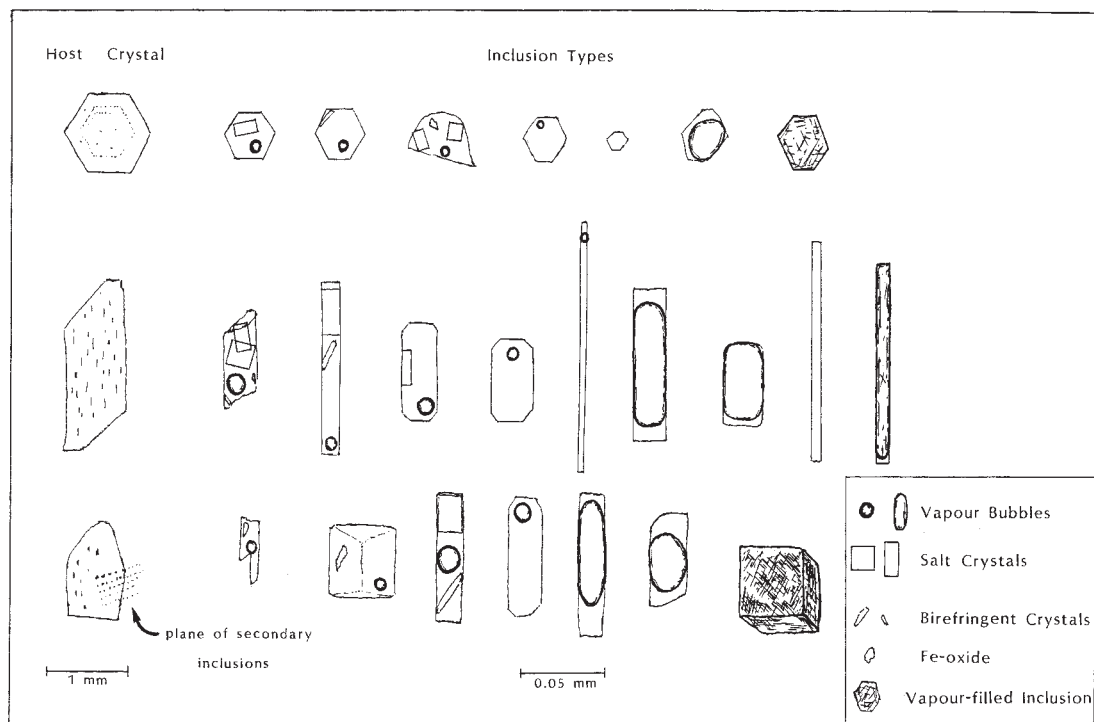


Fig. 7. Schematic representation of the range of fluid-inclusion types observed, shown with respect to the orientation of the host grain of apatite.

CO₂). However, double vapor bubbles were not observed at room temperature, nor was clathrate formation observed during sub-zero runs. This difficulty in detecting the carbonic phase may be a result of the very low $X(\text{CO}_2)$ (≤ 0.1) typical of these types of skarn (see above). Only a few type-I inclusions homogenized, between 250 to 350°C, before decrepitating. Halite-bearing inclusions also decrepitated before homogenization, and in no case did the salt crystal dissolve before decrepitation.

Sub-zero data for type-I and type-II inclusions did not differ significantly. First melting was observed between -60° and -40°C . Final ice melting took place between -23° and -35°C . These data indicate the presence of solutes other than NaCl. CaCl₂ is the most likely candidate for one of the other salts, as the eutectic of the H₂O–NaCl–CaCl₂ system occurs at -52°C (Linke 1958). The fluid composition may actually be more complex, as suggested by first melting observed at -60°C . The final ice-melting data correspond to average salinities of 30 wt.% NaCl equivalent (Potter *et al.* 1978). However, these salinities should be considered minimum estimates because of the presence of halite in type-III inclusions. In addition, halite saturation and a CaCl₂/NaCl weight ratio greater than about 1 (deter-

TABLE 2. SUMMARY OF FLUID-INCLUSION MICROTHERMOMETRIC DATA, ZENITH DEPOSIT, RENFREW DISTRICT, ONTARIO

Phase Change	Range	Peak	<i>n</i>
Type I			
Td	320 to 400°C	350°C	65
Th	250 to 350°C	300°C	23
Th daughter mineral	—	—	—
Te	-60 to -40°C	-50°C	33
Tm ice salinity ¹	-35 to -23°C	-20°C	67
		30	
Type II			
Td	350 to 430°C	380°C	32
Th	230 to 360°C	300°C	9
Te	-55 to -42°C	-50°C	8
Tm ice salinity ¹	-32 to -25°C	-20°C	12
		30	
principal cations	Na, Ca (Mg, Fe, K?)		
principal anion	Cl		
trapping T ²	500°–550°C		

Td: decrepitation temperature; Th: homogenization temperature; Te: eutectic temperature; Tm: final melting temperature.

¹ Salinity expressed in wt.% NaCl equivalents.

² Pressure corrected (as calculated with FLINCOR, Brown & Lamb 1989).

mined from final ice-melting temperature), constrains these inclusions to contain roughly 45 wt.% CaCl₂ (*cf.* Williams-Jones & Samson 1990). Microthermometric data are summarized in Table 2.

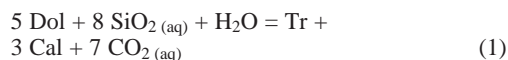
PRESSURE AND TEMPERATURE DURING SKARN FORMATION

The metasedimentary rocks in the Renfrew area have undergone metamorphism to the upper amphibolite facies (Easton 2000), corresponding to a temperature of 600° to 700°C and a pressure of around 700 MPa (*e.g.*, Streepey *et al.* 1997). Because the Mo-bearing skarns postdate deformation (see above), these conditions represent maximum estimates of the country-rock pressure and temperature at the time of igneous activity. After a period of tectonic quiescence of some 30–80 Ma (see above), the metasedimentary rocks were certainly at significantly lower P and T than those of peak metamorphism at the time of granite intrusion. On the basis of eutectic equilibria for H₂O-saturated haplogranite and the fluorine content of the rocks, Lentz & Fowler (1992) estimated that the crystallization of pegmatites and aplites in this part of the Grenville Province took place at ~600°C and confining pressures of 300 to 400 MPa. The almost monomineralic character of the skarns studied and the absence of diagnostic minerals preclude an independent estimate of the local P–T conditions. Therefore, it is assumed that pressure and temperature prevailing during pegmatite emplacement represent the upper limits for the conditions existing during skarn formation. A pressure correction of 300 to 400 MPa on the homogenization temperature of the fluid inclusions corresponds to trapping temperatures of about 500°–550°C. Although these are approximations, temperatures between 500 to 600°C and pressures of 300 to 500 MPa are typical conditions reported for similar skarns (*e.g.*, Bowman & Essene 1984, Keith *et al.* 1989, Meinert 1992, Lentz 1998b).

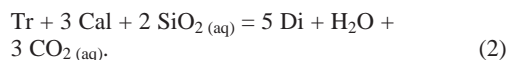
MINERAL AND FLUID EQUILIBRIA

The process advocated for endoskarn formation is one of infiltration of Ca, Mg and Fe into the granite (Einaudi & Burt 1982). Fe is enriched at and near the intrusive contact, and is reflected by the abundant sulfide mineralization and the Fe content of diopside (darker diopside occurs in proximal skarn). In distal assemblages the Fe/Mg decreases, which is reflected by the Fe content in diopside (*cf.* Table 1). This pattern is observed in reduced magnesian skarns with low to moderate $f(S_2)$ (*i.e.*, Po–Py) (*e.g.*, Gamble 1982, Lentz 1998).

The mineralogical zonation observed in exoskarn, from the marble contact toward the granite, consists of marble, tremolite + carbonate or quartz, and diopside with tremolite inclusions. This sequence indicates progressive addition of silica to the protolith and can be represented by the reactions:



and



According to reaction 1, calcite should be expected to precipitate in the tremolite zone. Although hydrothermal carbonate was observed in the tremolite zone, it is commonly not present in a three-to-one proportion with tremolite as expected. One possible explanation is that the skarn-forming fluid was locally undersaturated with respect to calcite.

The presence of tremolite relics in diopside, observed in the rock closest to the intrusive body, suggests that the reaction producing tremolite (1) preceded the formation of diopside (2) in this zone. Further away from the intrusion, in the tremolite zone, reaction 2 did not take place, as indicated by the absence of diopside. The skarn mineralogy thus indicates that the chemical potential of SiO₂, $\mu(\text{SiO}_2)$, decreases away from the intrusive contact, and, consequently, that the silica required to drive the above reactions to the right was supplied by the intrusive body. The association of pegmatites with aplites and the presence of a graphic texture observed in the granitic bodies related to the skarns (see above) are consistent with evolution of an aqueous fluid near the end of crystallization (Jahns & Burnham 1969, Lentz & Fowler 1992, London 1992). Under magmatic conditions (P = 300 MPa, T = 650°C), an aqueous fluid can transport up to ~1.5 wt.% SiO₂ in solution (*e.g.*, Anderson & Burnham 1967). Advective mass-transfer through such a fluid could, therefore, have introduced sufficient silica to produce the observed assemblages.

The fluid-inclusion study revealed two important physicochemical characteristics of the metasomatizing fluid: 1) it was immiscible with respect to H₂O and CO₂, and 2) it contained dissolved salts. Addition of important amounts of a third component (NaCl) to the system H₂O–CO₂ has the effect of raising its miscibility gap in T–X space (Bowers & Helgeson 1983a) well within the temperature range suggested for skarn formation, thus affecting the shape of mineral-stability fields and reaction curves. Modeling mineral equilibria in such a system requires the addition of a third dimension to conventional T–X(CO₂) binary diagrams. A schematic isothermal section through such a prism is depicted in Figure 8. This illustration shows how addition of salt can cause immiscibility to occur: the fluid composition moves away from the H₂O–CO₂ binary join, where the fluid is supercritical, into the liquid + vapor region, where tie-lines join the compositions of (H₂O + NaCl)-rich liquids coexisting with CO₂-rich vapors. A pseudobinary T–X(CO₂) section through Figure 8, for pressure and temperature conditions near those esti-

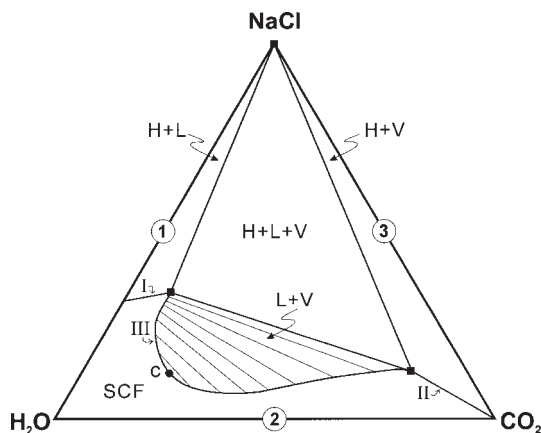


Fig. 8. Schematic phase-diagram from the ternary system $\text{H}_2\text{O}-\text{CO}_2-\text{NaCl}$ at a given $P-T$ (after Trommsdorff & Skippen 1986). Binary and ternary assemblages are labeled with Arabic and Roman numbers, respectively. H: halite, L: liquid, V: vapor, SCF: supercritical fluid, c: consolute point.

rated for the Zenith skarns, is depicted in Figure 9 (reactions corresponding to the univariant curves are shown in Table 3). This plot shows that the fluid behaved non-ideally at $X(\text{CO}_2)$ as low as ~ 0.15 , or probably even lower in view of the high salinity of the metasomatic fluid (*cf.* Bowers & Helgeson 1983b).

A possible path in $T-X(\text{CO}_2)$ space for a cooling orthomagmatic fluid is illustrated in Figure 9. The absence of wollastonite, forsterite and talc from the skarn parageneses limits the temperature for skarn formation to the fields labeled I and II, which is consistent with the estimates proposed above (500–550°C). Formation of the diopside zone in proximal skarn can take place at conditions defined by field I in Figure 9. The mineralogical changes occurring in response to the increasing $\mu(\text{SiO}_2)$ can be monitored on a $\text{SiO}_2-\text{CaO}-\text{MgO}$ compositional plot (Fig. 10). Silica-saturated fluids are represented by the SiO_2 apex of the triangle. Marble composition plots on the calcite–dolomite join, or slightly above it, to account for minor amounts of SiO_2 present prior to skarn formation. The country rock, equilibrating in response to the introduction of SiO_2 -rich fluid, changed its composition along a line joining the marble's bulk composition to the SiO_2 apex. This shift causes reactions (1) and (2) to occur, successively, with formation of tremolite first, and then, replacing it, diopside. In Figure 10 are indicated the aqueous silica contents of a fluid at equilibrium with the various mineral assemblages [at 550°C, 300 MPa and $X(\text{CO}_2) = 0.15$]. A compositional field where diopside is the only stable phase between quartz and dolomite exists on the CO_2 -rich side of the $T-X(\text{CO}_2)$ diagram in Figure 9 (not

TABLE 3. STABLE REACTIONS AMONG THE PHASES CALCITE, DIOPSIDE, DOLOMITE, FORSTERITE, QUARTZ, TALC, TREMOLITE AND WOLLASTONITE

a	3 Dol + 4 Qtz + H_2O	=	Tlc + 3 Cal + 3 CO_2
b	6 Cal + 4 Qtz + 5 Tlc	=	3 Tr + 2 H_2O + 6 CO_2
c	3 Cal + 2 Tlc	=	Tr + Dol + H_2O + CO_2
d	Tr + 2 Qtz + 3 Cal	=	5 Di + 3 CO_2 + H_2O
e	11 Dol + Tr	=	8 Fo + 13 Cal + H_2O + 9 CO_2
f	5 Cal + 3 Tr	=	2 Fo + 11 Di + 3 H_2O + 5 CO_2
g	Cal + Qtz	=	Wo + CO_2

Lettering refers to similarly labeled curves on Figure 9. The mineral symbols are those of Kretz (1983).

shown); however, this paragenesis was probably not important in view of the evidence for tremolite formation before diopside, and of the excessive CO_2 content of the fluids required [typical $X(\text{CO}_2)$ values in infiltrative magmatic skarn fluids reported in the literature are between 0.01 and 0.1; *e.g.*, Kerrick (1977), Taylor & O'Neil (1977), Bowman & Essene (1984), Bowman *et al.* (1985), Kwak (1986)].

As mentioned above, reaction (2) did not occur in the tremolite zone. As the fluid infiltrated further into the host rock and cooled, the bulk composition crossed a reaction surface into field II in Figure 9. Here, diopside is not stable, and tremolite is the only calc-silicate more stable than quartz plus dolomite. Alternatively, it could be envisaged that the silica activity of the fluid was never sufficiently high to move the composition of the rock to the diopside-present field of the triangle in Figure 10.

CONTROLS ON MOLYBDENITE MINERALIZATION

In the Zenith as well as in the other deposits visited, Mo mineralization is in the form of molybdenite flakes. Even though Ca activity must have been high in the mineralizing fluid, powellite (CaMoO_4) was not found. This absence can be explained by the relatively low $f(\text{O}_2)$ in the fluid, as indicated by the association of pyrite and pyrrhotite with molybdenite, plus the presence of CO_2 , both of which inhibit the formation of this phase (Hsu 1977, Darling 1994).

Field observations have shown that in all occurrences studied, molybdenite is spatially restricted to the skarns. It follows that molybdenum was transported in solution by the metasomatizing fluid. As discussed earlier, this fluid probably exsolved during pegmatite emplacement, which is consistent with the findings of Burrows & Spooner (1987) that processes of magmatic fractionation can increase substantially the Mo content of a parental granitic source. The fluid was rich in dissolved salts and immiscible. Although Mo partitions strongly into the aqueous fluid during melt–fluid separation, this process does not depend on the halogen content (Candela & Holland 1984, Keppler & Wyllie 1991). Therefore, despite the elevated salinity of the fluid, chloride

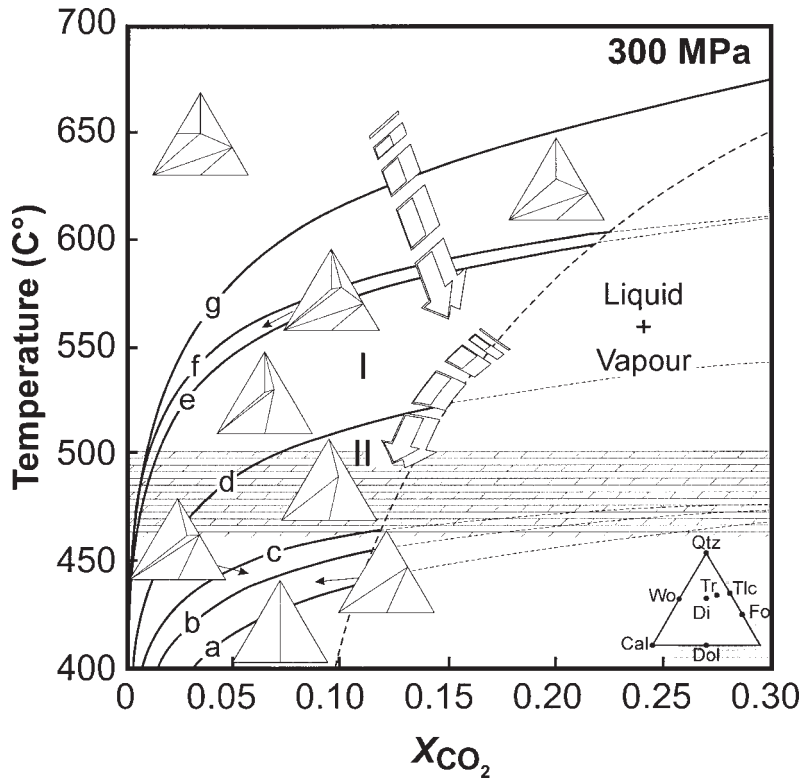


FIG. 9. Temperature- $X(\text{CO}_2)$ diagram depicting equilibria in the system $\text{SiO}_2\text{-CaO-MgO-NaCl-C-O-H}$ at 300 MPa (plotted using the TWQ software of Berman 1988). The hatched area is an estimate of the host-rock temperature. The large arrows indicate a cooling path for a fluid exsolved from a granitic pegmatite, whereas fields labeled I and II are possible $T\text{-}X(\text{CO}_2)$ domains for the formation of diopside and tremolite skarn zones, respectively. The compositional triangles indicate stable parageneses. Letters on reaction curves refer to the appropriate reaction in Table 3. For clarity, only reactions involving the calcite-dolomite-quartz compositional triangle are shown. The dashed curve is an estimate of the $\text{H}_2\text{O-CO}_2\text{-NaCl}$ miscibility gap for 35 wt.% NaCl [$X(\text{NaCl}) = 0.0715$; after Bowers & Helgeson (1983b)]. This diagram represents a section crossing the L + V field (III) of the ternary diagram in Figure 8.

complexing was probably not effective in transporting Mo. However, since boiling partitions H_2 into the vapor, the metasomatic fluid was likely relatively alkaline. Under these conditions, oxyacid complexing of Mo is favored, such as H_2MoO_4^0 , or, in view of the elevated content of alkalis, NaHMoO_4^0 and KHM o_4^0 , which have been shown to permit significant transport of this metal in solution (*e.g.*, Kudrin 1986, 1989, Wood *et al.* 1987).

A decrease in oxygen fugacity could destabilize oxyacidic complexes. It is plausible that conditions were reducing after the fluid reacted with the graphite-bearing marble. In addition, reduction of orthomagmatic SO_2 would increase H_2S (and HS^-) activity, thus triggering molybdenite precipitation.

SUMMARY AND CONCLUSIONS

The skarn at the Zenith Mo deposit, as well as other similar skarns in the Renfrew area of the Composite Arc Belt of the southwestern Grenville Province, occur at the contact between marble and post-tectonic granitic pegmatites. A prominent zonation developed in the skarn from the intrusive contact into the metasedimentary rock; it consists of diopside-bearing endoskarn plus diopside-dominated exoskarns, giving way to tremolite-dominated skarn. Metasomatism is interpreted to have occurred in response to infiltration into the marble of an aqueous fluid derived from the granitic pegmatites. Fluid inclusions that sampled the metasomatic fluid were found defining growth zones within apatite crystals

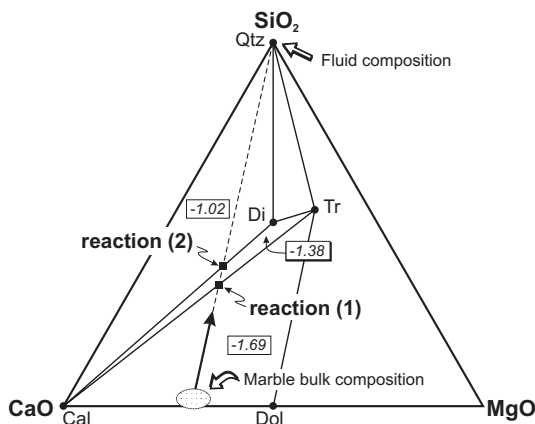


FIG. 10. Compositional $\text{SiO}_2\text{-CaO-MgO}$ (+ H_2O , CO_2) plot showing mineral equilibria in the field marked I in Figure 9. Schematically, the bulk compositions of the marble and of the orthomagmatic fluid also are shown as well as, in italic numerals, equilibrium concentrations of aqueous silica [expressed as $\log m(\text{H}_4\text{SiO}_4)^0$ for the assemblages Cal-Dol-Tr, Cal-Di-Tr and Cal-Di-Qtz (calculated for 550°C , 300 MPa , and $X(\text{CO}_2) = 0.15$; thermodynamic data from Kerrick & Jacobs 1981, Shvarov & Bastrakov 1999). The dashed line indicates the path along which the composition of the skarn evolved owing to SiO_2 introduction in marble, causing the succession of reactions (1) and (2) in the diopside zone.

in skarn. The fluid has a high salinity, is Ca-rich, and was immiscible at the time of trapping. In the diopside zone, introduction of silica into the marble via the aqueous fluid caused formation of tremolite, which was replaced by diopside as the $a(\text{SiO}_2)$ of the rock increased with increasing water:rock ratio. Mineral assemblages in the $\text{SiO}_2\text{-CaO-MgO-C-O-H}$ system that are compatible with this model can be found at pressure, temperature, $X(\text{CO}_2)$ that are consistent with the conditions that seem to have prevailed during skarn formation [$500^\circ\text{-}600^\circ\text{C}$, $300\text{-}400\text{ MPa}$, $X(\text{CO}_2) \approx 0.1$]. However, the absence of diopside in the tremolite zone indicates that during formation of the more distal skarns, the fluid was in a P-T- $X(\text{CO}_2)$ window where the dehydration decarbonation reaction $\text{Tr} + \text{Cal} \rightarrow \text{Di}$ (Reaction 2) does not occur.

Molybdenum mineralization in the skarn can be explained by metal transport in the metasomatic fluid by alkali oxyacidic complexing, followed by destabilization of these aqueous species and subsequent precipitation of molybdenite in response to a decrease in $f(\text{O}_2)$ and an increase in proportions of reduced sulfur upon reaction of the orthomagmatic fluid with the carbonaceous metasediments.

ACKNOWLEDGEMENTS

I thank Professor George Skippen for guidance, encouragement and critical assessments during the course of my B.Sc. thesis project at Carleton University, which constitutes part of this research. I am also indebted to Dave Lentz, who introduced me to the field area (and to charred barbecued ribs on the same occasion), provided help and discussion in the field as well as throughout my B.Sc. project. This manuscript also benefitted from discussions with B. Moine and critical reviews of Dan Kontak, David Lentz, Robert Linnen and Robert F. Martin.

REFERENCES

- ANDERSON, G.M. & BURNHAM, C.W. (1967): Reactions of quartz and corundum with aqueous chloride and hydroxide solutions at high temperatures and pressures. *Am. J. Sci.* **265**, 12-27.
- BERMAN, R.B. (1988): Internally-consistent thermodynamic data for minerals in the system $\text{Na}_2\text{O-K}_2\text{O-CaO-MgO-FeO-Fe}_2\text{O}_3\text{-Al}_2\text{O}_3\text{-SiO}_2\text{-TiO}_2\text{-H}_2\text{O-CO}_2$. *J. Petrol.* **29**, 445-522.
- BOWERS, T.S. & HELGESON, H.C. (1983a): Calculation of the thermodynamic and geochemical consequences of non ideal mixing in the system $\text{H}_2\text{O-CO}_2\text{-NaCl}$ on phase relations in geologic systems: equation of state for $\text{H}_2\text{O-CO}_2\text{-NaCl}$ fluids at high pressures and temperatures. *Geochim. Cosmochim. Acta* **47**, 1247-1275.
- _____ & _____ (1983b): Calculation of the thermodynamic and geochemical consequences of nonideal mixing in the system $\text{H}_2\text{O-CO}_2\text{-NaCl}$ on phase relations in geological systems; metamorphic equilibria at high pressures and temperatures. *Am. Mineral.* **68**, 1059-1075.
- BOWMAN, J.R. & ESSENE, E.J. (1984): Contact skarn formation at Elkhorn, Montana. I. P-T-component activity conditions of early skarn formation. *Am. J. Sci.* **284**, 597-650.
- _____, O'NEIL, J.R. & ESSENE, E.J. (1985): Contact skarn formation at Elkhorn, Montana. II. Origin and evolution of C-O-H skarn fluids. *Am. J. Sci.* **285**, 621-660.
- BROWN, P.E. & LAMB, W.M. (1989): P-V-T properties of fluids in the system $\text{H}_2\text{O} \pm \text{CO}_2 \pm \text{NaCl}$: new graphical presentations and implications for fluid inclusion studies. *Geochim. Cosmochim. Acta* **53**, 1209-1221.
- BURROWS, D.R. & SPOONER, E.T. (1987): Generation of a magmatic $\text{H}_2\text{O-CO}_2$ fluid enriched in Mo, Au, and W within an Archean sodic granodiorite stock, Mink Lake, northwestern Ontario. *Econ. Geol.* **82**, 1931-1957.
- BURT, D.M. (1982): Skarn deposits - historical bibliography through 1970. *Econ. Geol.* **77**, 755-763.

- CANDELA, P.A. & HOLLAND, H.D. (1984): The partitioning of copper and molybdenum between silicate melts and aqueous fluids. *Geochim. Cosmochim. Acta* **48**, 373-380.
- CARR, S.D., EASTON, R.M., JAMIESON, R.A. & CULSHAW, N.G. (2000): Geologic transect across the Grenville Orogen of Ontario and New York. *Can. J. Earth Sci.* **37**, 193-216.
- CARTER, T.C., COLVINE, A.C. & MEYN, H.D. (1980): Geology of base metal, precious metal, iron, and molybdenum deposits in the Pembroke–Renfrew area. *Ont. Geol. Surv., Mineral Deposits Circ.* **20**.
- DARLING, R.S. (1994): Fluid inclusion and phase equilibrium studies at the Cannivan Gulch molybdenum deposit, Montana, USA: effect of CO₂ on molybdenite–powellite stability. *Geochim. Cosmochim. Acta* **58**, 749-760.
- DAVIDSON, A. (1986): New interpretations in the southwestern Grenville Province. In *The Grenville Province* (J.M. Moore, Jr., A. Davidson & A.J. Baer, eds.). *Geol. Assoc. Can., Spec. Pap.* **31**, 61-74.
- DIPPLE, G.M. & GERDES, M.L. (1998): Reaction–infiltration feedback and hydrodynamics at the skarn front. In *Mineralized Intrusion-Related Skarn Systems* (D.R. Lentz, ed.). *Mineral. Assoc. Can., Short Course* **26**, 71-97.
- EASTON, R.M. (1986): Geochronology of the Grenville Province. In *The Grenville Province* (J.M. Moore, Jr., A. Davidson & A.J. Baer, eds.). *Geol. Assoc. Can., Spec. Pap.* **31**, 127-173.
- _____ (2000): Metamorphism of the Canadian Shield, Ontario, Canada. II. Proterozoic metamorphic history. *Can. Mineral.* **38**, 319-344.
- _____, CARTER, T.R. & SPRINGER, J.S. (1986): Mineral deposits of the Central Metasedimentary Belt, Grenville Province, Ontario and Quebec. *Geol. Assoc. Can. – Mineral. Assoc. Can., Ottawa '86, Field Trip Guidebook* **3**.
- EINAUDI, M.T. & BURT, D.M. (1982): Introduction – terminology, classification and composition of skarn deposits. *Econ. Geol.* **77**, 745-754.
- _____, MEINERT, L.D. & NEWBERRY, R.J. (1981): Skarn deposits. *Econ. Geol., 75th Anniv. Vol.*, 317-391.
- FOWLER, A.D. & DOIG, R. (1983): The age and origin of Grenville Province uraniumiferous granites and pegmatites. *Can. J. Earth Sci.* **20**, 92-104.
- GAMBLE, R.P. (1982): An experimental study of sulfidation reactions involving andradite and hedenbergite. *Econ. Geol.* **77**, 784-797.
- GRANT, W.T., PAPERTZIAN, V.C. & KINGSTON, P.W. (1989): Geochemistry of Grenville marble in southern Ontario. *Ont. Geol. Surv., Mineral Deposits Circ.* **28**.
- HSU, L.C. (1977): Effects of oxygen and sulfur fugacities on the scheelite–tungstenite and powellite–molybdenite stability relations. *Econ. Geol.* **72**, 664-670.
- JAHNS, R.H. & BURNHAM, C.W. (1969): Experimental studies of pegmatite genesis. I. A model for the derivation and crystallization of granitic pegmatites. *Econ. Geol.* **64**, 843-864.
- JOHNSTON, F.J. (1968): Molybdenum deposits of Ontario. *Ont. Dep. Mines, Mineral Resources Circ.* **7**.
- KARVINEN, W.O. (1973): *Metamorphic Molybdenite Deposits of the Grenville Province*. Ph.D. thesis, Queen's Univ., Kingston, Ontario.
- KEITH, J.D., VAN MIDDELAAR, W., CLARK, A.H. & HODGSON, C.J. (1989): Granitoid textures, compositions, and volatile fugacities associated with the formation of tungsten-dominated skarn deposits. In *Ore Deposition Associated with Magmas* (J.A. Whitney & A.J. Naldrett, eds.). *Rev. Econ. Geol.* **4**, 235-250.
- KEPLER, H. & WYLLIE, P.J. (1991): Partitioning of Cu, Sn, Mo, W, U, and Th between melt and aqueous fluid in the system haplogranite–H₂O–HCl and haplogranite–H₂O–HF. *Contrib. Mineral. Petrol.* **109**, 139-150.
- KERRICK, D.M. (1977): The genesis of zoned skarns in the Sierra Nevada, California. *J. Petrol.* **18**, 144-181.
- _____ & JACOBS, G.K. (1981): A modified Redlich–Kwong equation for H₂O, CO₂ and H₂O–CO₂ mixtures at elevated pressures and temperatures. *Am. J. Sci.* **281**, 735-767.
- KRETZ, R. (1983): Symbols for rock-forming minerals. *Am. Mineral.* **68**, 277-279.
- KUDRIN, A.V. (1986): The solubility of tugarinovite MoO₂ in aqueous solutions at elevated temperatures. *Geochem. Int.* **23**, 126-138.
- _____ (1989): Behavior of Mo in aqueous NaCl and KCl solutions at 300–450°C. *Geochem. Int.* **28**, 87-99.
- KWAK, T.A.P. (1986): Fluid inclusions in skarns (carbonate replacement deposits). *J. Metamorph. Geol.* **4**, 363-384.
- LENTZ, D.R. (1996): U, Mo, and REE mineralization in late-tectonic granitic pegmatites, southwestern Grenville Province, Canada. *Ore Geol. Rev.* **11**, 197-227.
- _____ (1991): U-, Mo-, and REE-bearing pegmatites, skarns, and veins in the Central Metasedimentary Belt, Grenville Province, Ontario. *Geol. Assoc. Can. – Mineral. Assoc. Can., Field Trip Guidebook* **A9**.
- _____, ed. (1998a): Mineralized intrusion-related skarn systems. *Mineral. Assoc. Can., Short Course* **26**.
- _____ (1998b): Late-tectonic U–Th–Mo–REE skarn and carbonatitic vein-dyke systems in the southwestern Grenville Province: a pegmatite-related pneumatolytic model linked to marble melting (limestone syntexis). In *Mineralized Intrusion-Related Skarn Systems* (D.R. Lentz, ed.). *Mineral. Assoc. Can., Short Course* **26**, 519-657.
- _____ & FOWLER, A.D. (1992): A dynamic model for graphic quartz–feldspar intergrowths in granitic pegmatites

- in the southwestern Grenville Province. *Can. Mineral.* **30**, 571-585.
- _____ & SUZUKI, K. (2000): A low-F, pegmatite-related Mo skarn from the southwestern Grenville Province, Ontario, Canada: phase equilibria and petrogenetic implications. *Econ. Geol.* **95**(6), in press.
- LINKE, W.F. (1958): *Solubilities. Inorganic and Metal-Organic Compounds I* (4th ed). Van Nostrand Reinhold, New York, N.Y.
- LONDON, D. (1992): The application of experimental petrology to the genesis and crystallization of granitic pegmatites. *Can. Mineral.* **30**, 499-540.
- LUMBERS, S.B. (1982): Summary of metallogeny, Renfrew County area. *Ont. Geol. Surv., Rep.* **212**.
- MALCZAK, J., CARTER, T.C. & SPRINGER, J.S. (1985): Base metal, molybdenum, and precious metal deposits, Madoc-Sharbot Lake areas, southeastern Ontario. *Ont. Geol. Surv., Open File Rep.* **5548**.
- MEINERT, L.D. (1992): Skarns and skarn deposits. *Geosci. Can.* **19**, 145-162.
- _____ (1997): Application of skarn deposit zonation models to mineral exploration. *Expl. Mining Geol.* **6**, 185-208.
- PAN, YUANMING (1998): Scapolite in skarn deposits: petrogenetic and geochemical significance. In *Mineralized Intrusion-Related Skarn Systems* (D.R. Lentz, ed.). *Mineral. Assoc. Can., Short Course* **26**, 169-209.
- POTTER, R.W., II, CLYNNE, M.A. & BROWN, D.L. (1978): Freezing point depression of aqueous sodium chloride solutions. *Econ. Geol.* **73**, 284-285.
- QUINN, H.A. (1952): Renfrew map-area, Renfrew and Lanark counties, Ontario. *Geol. Surv. Can., Pap.* **51-27**.
- RAY, G.E. & WEBSTER, I.C.L. (1991): An overview of skarn deposits. In *Ore Deposits, Tectonics and Metallogeny in the Canadian Cordillera*. *B.C. Ministry Energy, Mines, Petrol. Resources, Pap.* **1991-4**, 213-252.
- ROEDDER, E. (1984): Fluid inclusions. *Rev. Mineral.* **12**.
- SATTERLY, J. (1957): Radioactive mineral occurrences in the Bancroft area. *Ontario Dep. Mines, LXV*(6).
- SHVAROV, YU.V. & BASTRAKOV, E.N. (1999): HCh: a software package for geochemical equilibrium modelling. User's Guide. *Aust. Geol. Surv. Organisation, Record* **1999/25**.
- STREEPEY, M.M., ESSENE, E.J. & VAN DER PLUJM, B.A. (1997): A compilation of thermobarometric data from the Metasedimentary Belt of the Grenville Province, Ontario and New York State. *Can. Mineral.* **35**, 1237-1247.
- TAYLOR, B.E. & O'NEIL, J.R. (1977): Stable isotope studies of metasomatic Ca-Fe-Al-Si skarns and associated metamorphic and igneous rocks, Osgood Mountains, Nevada. *Contrib. Mineral. Petrol.* **63**, 1-49.
- TROMMSDORFF, V. & SKIPPEN, G.B. (1986): Vapor loss ("boiling") as a mechanism for fluid evolution in metamorphic rocks. *Contrib. Mineral. Petrol.* **94**, 317-322.
- VOKES, F. (1963): Molybdenum deposits of Canada. *Geol. Surv. Can., Econ. Geol. Rep.* **20**.
- WERRE, R.W., JR., BODNAR, R.J., BETHKE, P.M. & BARTON, P.B., JR. (1979): A novel gas-flow fluid inclusion heating/freezing stage. *Geol. Soc. Am., Abstr. Programs* **11**, 539.
- WILLIAMS-JONES, A.E. & SAMSON, I.M. (1990): Theoretical estimation of halite solubility in the system NaCl-CaCl₂-H₂O; applications to fluid inclusions. *Can. Mineral.* **28**, 299-304.
- WOOD, S.A., CRERAR, D.A. & BORCSIK, M.P. (1987): Solubility of the assemblage pyrite - pyrrhotite - magnetite - sphalerite - galena - gold - stibnite - bismuthinite - argentite - molybdenite in H₂O-NaCl-CO₂ solutions from 200°C to 350°C. *Econ. Geol.* **82**, 1864-1887.
- WYNNE-EDWARDS, H.R. (1972): The Grenville Province. In *Variations in Tectonic Styles in Canada* (R.A. Price & R.J.W. Douglas, eds.). *Geol. Assoc. Can., Spec. Pap.* **11**, 263-334.
- ZHARIKOV, V.A. (1970): Skarns. *Int. Geol. Rev.* **12**, 541-559, 619-647, 760-775.
- _____ (1991): Skarn types, formation and ore mineralization conditions. In *Skarns - their Genesis and Metallogeny* (K.A. Barto, ed.). Theophrastus Publications SA, Athens, Greece (455-466).

Received February 18, 1999, revised manuscript accepted June 6, 2000.